Journal of Hydronautics

VOLUME 5 APRIL 1971 NUMBER 2

Forces and Motions of a Flexible Floating Barrier

JEROME H. MILGRAM*
Massachussetts Institute of Technology, Cambridge, Mass.

The problems of determining the motions, the structural and the hydrodynamic forces on a flexible, floating barrier are considered. Such barriers are frequently used as containment devices for floating liquid pollutants such as oil. Local hydrodynamic forces on a barrier are approximated by those for a straight barrier at angles to the waves and current equal to those of the local section. This affords a simplification in the theory that allows a solution in closed form to the nonlinear problem of a barrier in a current and a numerical solution for the linearized problem of a barrier in waves. These problems are treated additively inasmuch as the interaction effects between waves and currents on a barrier are not yet known. The degree to which the barrier follows the fluid particle motion in waves is known to be particularly important. Poor following not only leads to degradation of the barrier as a containment device, but also results in enormous forces on the barrier. Application of the method of solution for barriers to the case of a towed cable in waves is discussed. Previously unpublished force coefficients for a two-dimensional flat plate are given.

Nomenclature

b = vertical distance from the middraft to the center of mass of the barrier
B_j = spring constant in the jth degree of freedom
C_d = steady current drag coefficient
c_j = wave force coefficient in the jth degree of freedom
c_j^n = c_j for waves at normal incidence
d = barrier draft
F^h = steady horizontal hydrodynamic force per unit length normal to the centerplane of the barrier due to a current
F^t = steady horizontal force per unit length normal to the centerplane of the barrier due to tension in the curved barrier
F_j^m = hydrodynamic force per unit length in the jth degree of freedom due to motion of the barrier
F_j^s = hydrostatic spring force per unit length in the jth degree of freedom
F_j^t = unsteady force per unit length in the jth degree of freedom due to tension in the barrier
F_j^w = wave force per unit length in the jth degree of freedom
k = circular wavenumber
$(\hat{i},\hat{j})$ = unit vectors in the x and y directions
L = barrier length
$\mathbf{n}$ = outward unit normal to the barrier
R_g = gap ratio: the ratio of the barrier opening width to the barrier length
T = tension
s = arc length parameter along the barrier
V = current speed
(x,y,z) = cartesian coordinate system with the x-y plane on the position of the undisturbed free surface and z positive upwards
(X^B,Y^B) = x,y coordinates of points on the barrier
(x_o^B,y_o^B) = x,y coordinates of points on the barrier in a steady current
(X_u^B,Y_u^B) = unsteady part of (X_j^B,Y^B)
$(X^+,Y^+),(X^-,Y^-),(X^s,Y^s)$ = barrier end point coordinates
α = the angle between the direction of wave propagation and the x axis
β_{ij} = barrier mass and inertia coefficients
ϵ = inverse tension parameter ($\epsilon = L^2\sigma^2/T^2$)
H = incident wave surface elevation
H_j = wave surface elevation due to barrier motion in the jth degree of freedom
ω = radian frequency
ψ_j = barrier displacement from its mean position in the jth degree of freedom
Θ = barrier tangent angle
θ_u = unsteady barrier tangent angle
θ_o = mean barrier tangent angle
σ = hydrodynamic force per unit length on a straight barrier normal to a steady current
τ = tension parameter ($\tau = T/L\sigma$)
μ_{jl} = hydrodynamic inertia coefficient in the jth degree of freedom due to motion in the lth degree of freedom
ν_{jl} = hydrodynamic damping coefficient in the jth degree of freedom due to motion in the lth degree of freedom

Received August 24, 1970; revision received November 25, 1970. The research reported in this paper was supported in part by the Federal Water Pollution Control Agency under Contract 15080 ESL.

* Associate Professor of Naval Architecture.

Subscripts

2 = sway
3 = heave
5 = roll about the middraft
8 = roll about the mean waterline

1. Introduction

DURING the past few years, a number of attempts have been made to contain floating oil slicks by means of a floating barrier. For most of these attempts, containment could not be achieved when currents exceeded one knot or waveheights exceeded a few inches. In order to achieve effective containment, oil must not pass over or under the barrier in significant quantities. Achievement of containment requires, in part, the solution and understanding of a number of interconnected mechanical problems. The details of how wind and currents drive oil against a barrier must be understood. Similarly, an understanding of the mechanics of current induced oil leakage under a barrier is required. Partial answers to these problems have been provided by Hoult[1] and Robbins.[2] The forces and moments on a surface-piercing barrier due to a current must be determined. Force and moment coefficients for the two-dimensional case have been determined by Robbins. Once the hydrodynamic forces on the barrier are known, the tension in the barrier must be determined, as this effects the dynamic response of the barrier in waves as well as the structural design. The solution to this tension problem is given in Sec. 2 of this paper. In the presence of water waves, the resulting forces on the barrier must be provided, and the effect of waves on oil containment must be determined. The latter effect is extremely complicated. The motion of the barrier and of the upper and lower surfaces of the oil slick at the barrier must be known to determine whether or not oil will pass under or over the barrier. In the case of slicks on coastal waters, both currents and waves are usually simultaneously present, further complicating the problem.

The problems treated in this paper are those of determining the forces on a barrier in deep water currents and waves and the resulting barrier configurations and motions. The solutions are by no means complete—much remains to be learned. In particular, details of the effects of the interactions of combined waves and currents on a barrier are unknown. Work in this area is presently in progress, and results are expected in the near future. For the present, the effects of waves and currents are treated additively. Although interaction effects on barrier forces and motions are certainly important, this paper, which omits these effects, is intended to serve two purposes. First, it provides a basis for initial studies on barrier mechanics and secondly, it provides equations and their method of solution which can be used for engineering purposes in the design of barriers as well as for estimating the extremes of conditions in which a given barrier can be effective.

Forces and motions of a barrier are determined here in terms of pertinent force coefficients. Knowledge of most of these coefficients at this time is limited to a single fluid with a free surface. An exception is the drag coefficient of a steady water current beneath an oil slick on a vertical plate that was determined experimentally by Robbins.[2]

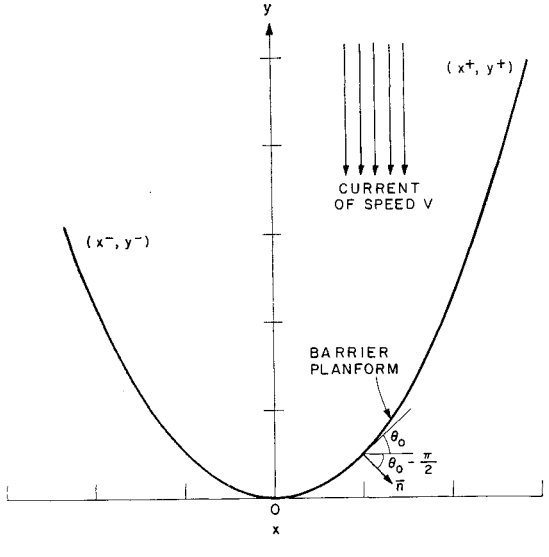

Fig. 1 Geometry for a barrier of length L in a steady current of speed V.

2. Barrier in a Steady Current

The problem considered here is that of a long barrier of length L in the presence of a current of speed V incident upon the barrier from the positive y direction, as shown in Fig. 1. The barrier is assumed to be completely flexible in bending and torsion. The origin of the xy coordinate system on the free surface is taken as that point on the barrier where the y coordinate is a minimum and the z axis is taken to be positive upwards. The graph of the barrier in the xy plane is given by

$$y_o^B = f(x) \tag{1}$$

One end of the barrier is at (x^-,y^-), and the other is at (x^+,y^+). The local angle between the x axis and the vector tangent to the barrier is denoted by θ_o. The positive normal direction is taken outward from the convex side (Fig. 1). It is assumed that the tangential component of the local hydrodynamic force is negligible compared to the normal hydrodynamic force, so that the tension T in the barrier is a constant. Also, it is assumed that the cross-sectional shape of the barrier is constant along the length of the barrier. If a cylinder, having this cross section and length L, has drag D when placed in a current of speed V at normal incidence, the drag coefficient of the barrier is defined as

$$C_d = D/(\tfrac{1}{2})\rho V^2 L d \tag{2}$$

where ρ is the density of the fluid and d is the draft of the barrier.

It has been shown by Eames[3] and Springston[4] that if an elongated body has a drag coefficient C_d when a current is normal to its longitudinal axis, it has a normal force coefficient of $C_d \cos^2\theta$ if the angle between the normal to the longitudinal axis and the current direction is θ. Although this result was determined in the absence of a free surface, it will be used here since free surface data is not available, and momentum transfer considerations indicate that this result should be nearly correct with or without a free surface. Thus the normal hydrodynamic force on the barrier, per unit length, is given by

$$F^h = \sigma/[1 + (df/dx)^2] \tag{3}$$

where

$$\sigma = (\tfrac{1}{2})\rho V^2 d C_d \tag{4}$$

The normal force, per unit length, due to the tension in the curved barrier is

$$F^t = -(Td^2f/dx^2)/[1 + (df/dx)^2]^{3/2} \tag{5}$$

For equilibrium, $F^h + F^t = 0$, which leads to the differential equation

$$Tf'' - \sigma[1 + (df/dx)^2]^{1/2} = 0 \tag{6}$$

which, for $f(0) = f'(0) = 0$, has the unique solution

$$f(x) = (T/\sigma)(\cosh\sigma x/T - 1) \tag{7}$$

Thus the barrier shape is a catenary. In order to determine the tension in the barrier, the condition that L is the arc length of the barrier between (x^-,y^-) and (x^+,y^+) is used. This condition requires that

$$(T/L\sigma)(\sinh\sigma x^+/T - \sinh\sigma x^-/T) = 1 \tag{8}$$

$T/L\sigma$ is called the tension parameter and is denoted by τ.

A common case is that for which the barrier configuration is symmetrical about the y axis. For this case

$$x^+ = -x^- \equiv x^s \tag{9}$$

$$y^+ = y^- \equiv y^s \tag{10}$$

and the gap ratio R_g is defined by

$$Rg = 2x^s/L \tag{11}$$

For this case,

$$\tau \sinh Rg/2\tau = \tfrac{1}{2} \tag{12}$$

Figure 2 shows a graph of the tension parameter τ as a function of R_g. Figure 3 shows barrier configurations for gap ratios between 0.1 and 0.95 for the case of $\sigma = 45$ slugs/sec.[2]

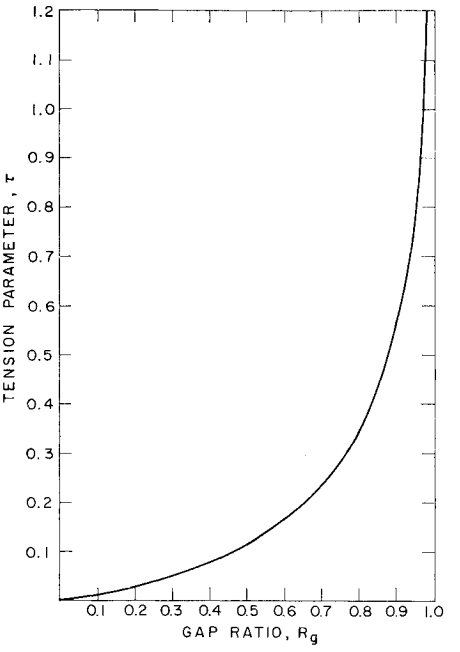

Fig. 2 Tension parameter τ as a function of the gap ratio R_g, as given by Eq. (12) for a barrier moored symmetrically with respect to a current.

3. Barrier in Waves and Current

When a barrier is in the presence of waves, there will almost always be a current with respect to the barrier. Sources of this current are ocean currents, tidal flow, Stokes' drift due to the waves, or the result of towing the barrier. Since the steady force on the barrier determines its mean configuration (Sec. 2), the effects of waves on a barrier must be considered with the simultaneous presence of a current.

The quantities to be estimated here are the unsteady forces on the barrier and the motions of the barrier. In carrying out these estimations, a number of simplifying assumptions are made. The condition considered is the combination of a plane monocromatic wave and a current. Linearized approximations for the wave effects are used so the effects of an arbitrary sea state can be determined by harmonic analysis.

The first simplifying assumption used is the neglect of the interaction of wave and current effects. It is assumed that the current determines the mean barrier configuration, as in Sec. 2, and that the waves cause an unsteady motion about this mean configuration. For the case of a plane wave, this results in unsteady forces and motions at the wave frequency when linearized theory is used. It is anticipated that interaction effects will occur at the harmonics of the wave frequency. These interaction effects are related to the unsteady flow separation at the bottom of the barrier. A further discussion of interaction effects appears in the Appendix.

The second simplifying assumption is that the hydrodynamic force per unit length acting on any cross section of the barrier depends only on the incident wave and current and the local position, orientation, and motion of the cross section. This approximation allows each section of the barrier to be treated as a section of a two-dimensional body at an arbitrary angle to the waves as far as hydrodynamic forces are concerned.

It is assumed that the unsteady motions are small compared to the wavelength, so that wave effects can be determined at the mean position of the barrier, and that the forces due to waves and barrier motions are linear in wave amplitude and barrier motion amplitude, respectively. In the absence of a current, it has been shown by Drake[5] that these assumptions are valid if the wave and motion amplitudes have orders of magnitude no larger than that of the cross-sectional dimensions of the barrier. Linearity of the forces due to motion, when the motion is not large compared to the barrier cross-sectional dimensions, can be anticipated from the work of Kuelegan and Carpenter,[6] who found that this was true in the absence of free surface effects.

The motions of the barrier will be denoted by the subscripts; 2 for sway, which is the horizontal motion of the barrier normal to its centerplane; 3 for heave; and 5 for roll about the middraft.

The positive direction of roll is that direction in which the upper portion of the barrier moves in the positive sway direction and the lower portion of the barrier moves in the negative sway direction. When forces and moments are discussed in general, they will be referred to as "forces." Inasmuch as monochromatic waves are being considered and linearity of the problem is assumed, all unsteady quantities will have a sinusoidal time dependence. These quantities will be denoted by upper case letters and their complex amplitudes will be denoted by corresponding lower case letters. The time dependence will be taken as $e^{i\omega t}$ and the real part operation will be implied in all complex expressions containing the time symbol t. As an example, a general quantity Q depending on space and time is represented as

$$Q(s,t) = q(s)e^{i\omega t} \tag{13}$$

c_2, c_3, and c_5 are the three complex wave-force coefficients where the complex amplitudes of the sway and heave forces per unit length on the barrier due to the wave are given by

$$f^w_j(s) = (\pi/2)\eta(s)c_j(s)\rho d^2\omega^2 \quad j = 2,3 \tag{14}$$

and the roll moment per unit length due to the wave is given by

$$f_5{}^w(s) = (\pi/4)\eta(s)c_5(s)\rho d^3\omega^2 \tag{15}$$

where $\eta(s)$ is the complex amplitude of the incident wave.

The motion of the barrier in one of its degrees of freedom will, in principle, result in hydrodynamic forces in all three degrees of freedom. However, only barrier cross sections that are symmetrical about their centerplanes will be considered, so that the cross coefficients between heave and other degrees of freedom are zero. The fluid forces on the barrier will be divided into zero frequency (hydrostatic) effects plus

frequency dependent effects, where the zero frequency effects are called "spring constants." Because of the assumed symmetry of the barrier sections, all cross spring constants are zero. The sway spring constant is zero, the heave spring constant is called B_3, and the roll spring constant is called B_5, where the associated heave force per unit length is

$$F_3^s(s,t) = -(\pi/2)\rho g d B_3 \Psi_3(s,t) \tag{16}$$

and the associated roll moment per unit length is

$$F_5^s(s,t) = -(\pi/4)\rho g d^3 B_5 \Psi_5(s,t) \tag{17}$$

Ψ_2 is the unsteady sway displacement normal to the centerplane, Ψ_3 is the unsteady heave displacement, and Ψ_5 is the unsteady roll angle.

The frequency dependent force in the jth degree of freedom due to motion in the lth degree of freedom has a component whose phase is opposite to the phase of the acceleration and a component whose phase is opposite to the phase of the velocity. Thus the complex amplitudes of the frequency dependent forces per unit length on the barrier, as a result of its motion, can be expressed as

$$f_2^m = (\pi/2)\rho d^2\omega^2(\mu_{22} - i\nu_{22})\psi_2 + (\pi/2)\rho d^3\omega^2(\mu_{25} - i\nu_{25})\psi_5 \tag{18}$$

$$f_3^m = (\pi/2)\rho d^2\omega^2(\mu_{33} - i\nu_{33})\psi_3 \tag{19}$$

$$f_5^m = (\pi/2)\rho d^3\omega^2(\mu_{52} - i\nu_{52})\psi_2 + (\pi/4)\rho d^4\omega^2(\mu_{55} - i\nu_{55})\psi_5 \tag{20}$$

μ_{jl} is called the inertia coefficient in the jth degree of freedom as a result of motion in the lth degree of freedom, and ν_{jl} is similarly called the damping coefficient.

Knowledge of the coefficients μ_{jl} and ν_{jl} for bodies with sharp lower edges presently exists for only a few cases in the absence of a steady current and knowledge of c_j only exists for a few such cases in the absence of a steady current and with the direction of wave propagation normal to the centerplane of the barrier. These coefficients, insofar as they apply to barriers, are given in the Appendix.

The only force acting on a section of the barrier that has not yet been considered is that due to the combined effect of tension and barrier displacement. The roll moment due to the combination of tension and barrier twist depends on how the tension is carried by the barrier. Frequently, the tension is carried in a strength member near the barrier middraft. This case, which is the one considered here, results in zero roll moment about the middraft because of the combination of tension and twist.

Sway and heave forces occur from the combination of tension and barrier curvature. The sway force is considered in detail. Here, s is the arc length parameter along the barrier, and points on the barrier are given by $[X^B(s,t), Y^B(s,t)]$:

$$X^B(s,t) = \int_{s_o}^{s} \cos\Theta(s',t)ds' + X^B(s_o,t) \tag{21}$$

$$Y^B(s,t) = \int_{s_o}^{s} \sin\Theta(s',t)ds' + Y^B(s_o,t) \tag{22}$$

Let Θ, the local barrier tangent angle, be decomposed into a mean value $\theta_o(s)$ and an unsteady component $\theta_u(s,t)$:

$$\Theta(s,t) = \theta_o(s) + \Theta_u(s,t) \tag{23}$$

θ_o is the tangent angle of the barrier due to the current and is obtained from Sec. 2 as

$$\theta_o = \tan^{-1}(df/dx) \tag{24}$$

The complex amplitude of the unsteady horizontal force normal to the barrier due to the tension T is

$$f_1^t = -T(d\theta_u/ds) \tag{25}$$

T is taken as constant in time, which is the case if the longitudinal elasticity of the barrier is large. It is assumed that $\theta_u \ll 1$ so that linearization in θ_u yields

$$X^B(s,t) = \int_{s_o}^{s} \cos\theta_o(s')ds' - \int_{s_o}^{s} \Theta_u(s',t) \times \sin\theta_o(s')ds' + X^B(s_o,t) \tag{26}$$

$$Y^B(s,t) = \int_{s_o}^{s} \sin\theta_o(s')ds' + \int_{s_o}^{s} \Theta_u(s',t) \times \cos\theta_o(s')ds' + Y^B(s_o,t) \tag{27}$$

The horizontal unit vector normal to the mean position of the barrier centerplane is

$$\bar{n}(s) = \hat{\imath}\sin\theta_o(s) - \hat{\jmath}\cos\theta_o(s) \tag{28}$$

Thus $\psi_2(s)$, the complex amplitude of the unsteady deflection of the barrier in the direction of $\bar{n}$, is

$$\psi_2(s) = -\sin\theta_o(s)\int_{s_o}^{s} \theta_u(s')\sin\theta_o(s')ds' - \sin\theta_o(s)x_u^B(s_0) - \cos\theta_o(s)\int_{s_o}^{s} \theta_u(s')\cos\theta_o(s')ds' - \cos\theta_o(s)y_u^B(s_o) \tag{29}$$

x_u^B and y_u^B are the complex amplitudes of the unsteady parts of X^B and Y^B. Differentiating this expression twice with respect to s gives

$$d\theta_u/ds = -d^2\psi_2/ds^2 + (d^2\theta_o/ds^2)(ds/d\theta_o) \times (d\psi_2/ds + \theta_u) - \psi_2(d\theta_o/ds)^2 \tag{30}$$

From the results of Sec. 2,

$$d\theta_o/ds = (\sigma/T)/\cosh^2\sigma x_o^B/T \tag{31}$$

and

$$d^2\theta_o/ds^2 = -2(\sigma/T)^2(\sinh\sigma x_o^B/T)/(\cosh^4\sigma x_o^B/T) \tag{32}$$

To consider Eq. (32) in terms of dimensionless quantities, let

$$\psi_1 = L\hat{\psi}_1 \tag{33}$$

$$x_o^B = L\hat{x}_o^B \tag{34}$$

$$s = L\hat{s} \tag{35}$$

$$1/\tau^2 = \epsilon \tag{36}$$

Then from Eqs. (30–36),

$$d\theta_u/d\hat{s} = -d^2\hat{\psi}_2/d\hat{s}^2 - \frac{2\epsilon^{1/2}\sinh\epsilon^{1/2}\hat{x}_o^B}{\cosh^2\epsilon^{1/2}\hat{x}_o^B} \times (d\hat{\psi}_2/ds + \theta_u) - \frac{\epsilon\hat{\psi}_2}{\cosh^4\epsilon^{1/2}\hat{x}_o^B} \tag{37}$$

The conditions of $\epsilon = 0$ corresponds to mean configuration of a straight line for which case Eq. (37) collapses to the usual equation for the linearized curvature. It is assumed that for values of ϵ encountered, $\hat{\psi}_2$ and $\hat{\psi}_u$ can be represented by expansions in powers of ϵ

$$\hat{\psi}_2 = \hat{\psi}_2^{(0)} + \epsilon\psi_2^{(1)} + \epsilon^2\psi_1^{(2)} + \dots \tag{38}$$

$$\theta_u = \theta_u^{(0)} + \epsilon\theta_u^{(1)} + \epsilon^2\theta_u^{(2)} + \dots \tag{39}$$

Eq. (37) is satisfied by Eqs. (38) and (39) and the following set of equations:

$$d\theta_u^{(0)}/d\hat{s} = -d^2\hat{\psi}_2^{(0)}/d\hat{s}^2 \tag{40}$$

$$d\theta_u^{(1)}/d\hat{s} = -d^2\hat{\psi}_2^{(1)}/d\hat{s}^2 - \hat{\psi}_2^{(0)} \tag{41}$$

$$d\theta_u^{(2)}/d\hat{s} = -d^2\psi_2^{(2)}/d\hat{s}^2 + \dots \tag{42}$$

. .
. .
. .

The complex amplitude of the sway force per unit length as a result of tension can be expanded as

$$f_1{}^t = -\sum_{j=0}^{\infty} T\epsilon^j \frac{d\theta_u{}^{(j)}}{ds} \tag{43}$$

All of the sway forces on the barrier have now been identified. It is anticipated that retaining only the first one or two terms in expansions in powers of ϵ will yield accurate results when ϵ is small. Figure 2 indicates ϵ is small when the gap ratio is large. Just how small ϵ must be for results to be accurate can only be determined by calculating the contributions to the solutions by a few powers of ϵ.

The nondimensional mass and inertia constants for the barrier, related to its own mass distribution, are denoted by β_{ij}. In particular, $(\pi/2)\rho d^2\,\beta_{22}$ is the mass per unit length of the barrier, $(\pi/4)\rho d^4\,\beta_{55}$ is the moment of inertia per unit length of the barrier $(\pi/2)\rho d^3\,\beta_{25}$ is the linear acceleration of the center of mass of a section of the barrier as a result of unit angular acceleration about the middraft, and $(\pi/2)\rho d^3\beta_{52}$ is the angular acceleration of the center of mass with respect to the middraft due to unit linear acceleration in sway. A well-known result from rigid body mechanics is that

$$\beta_{25} = \beta_{52} = \beta_{22}b/d \tag{44}$$

where b is the distance of the center of gravity above the middraft. Naturally,

$$\beta_{22} = \beta_{33} \tag{45}$$

The equations of sway motion for zero and first order in ϵ can then be constructed as

$$T\frac{d^2\psi_2{}^{(0)}}{ds^2} + (\pi/2)\rho d^2\omega^2(u_{22} + \beta_{22} - i\nu_{22})\psi_2{}^{(0)} + (\pi/2)\rho d^3\omega^2(u_{25} + \beta_{25} - i\nu_{25})\psi_5{}^{(0)} = -(\pi/2)\eta(s)c_2(s)\rho d^2\omega^2 \tag{46}$$

$$T\frac{d^2\psi_2{}^{(1)}}{ds^2} + (\pi/2)\rho d^2\omega^2(u_{22} + \beta_{22} - i\nu_{22})\psi_2{}^{(1)} + (\pi/2)\rho d^3\omega^2(u_{25} + \beta_{25} - i\nu_{25})\psi_5{}^{(1)} = -T\psi_2{}^{(0)}(s)/L^2 \tag{47}$$

where ψ_5 is expanded as

$$\psi_5 = \sum_{j=0}^{\infty} \epsilon^j \psi_5{}^{(j)} \tag{48}$$

and

$$\psi_2{}^{(j)} = L\hat{\psi}_2{}^{(j)} \tag{49}$$

The equations for roll motion are determined simply as

$$2(u_{52} + \beta_{52} - i\nu_{52})\psi_2{}^{(0)} + d[u_{55} + \beta_{55} - (g/\omega^2 d)\beta_5 - i\nu_{55}]\psi_5{}^{(0)} = -\eta(s)c_5(s) \tag{50}$$

and

$$2(u_{52} + \beta_{52} - i\nu_{52})\psi_2{}^{(1)} + d[u_{55} + \beta_{55} - (g/\omega^2 d)\beta_5 - i\nu_{55}]\psi_5{}^{(1)} = 0 \tag{51}$$

From Eqs. (46) and (50)

$$\frac{d^2\psi_2{}^{(0)}}{ds^2} + \frac{(\pi/2)\rho d^2\omega^2}{T}\left[u_{22} + \beta_{22} - i\nu_{22} - \frac{2(u_{52} + \beta_{52} - i\nu_{52})(u_{25} + \beta_{25} - i\nu_{25})}{(u_{55} + \beta_{55} - \{g/\omega^2 d\}\beta_5 - i\nu_{55})}\right]\psi_2{}^{(0)} = -\frac{(\pi/2)\eta(s)\rho d^2\omega^2}{T} \times \left[c_2(s) - c_5(s)\frac{(u_{25} + \beta_{25} - i\nu_{25})}{(u_{55} + \beta_{55} - \{g/\omega^2 d\}B_5 - i\nu_{55})}\right] \tag{52}$$

and from Eqs. (47) and (51)

$$\frac{d^2\psi_2{}^{(1)}}{ds^2} + \frac{(\pi/2)\rho d^2\omega^2}{T}\left[u_2 + \beta_{22} - i\nu_{22} - \frac{2(u_{52} + \beta_{52} - i\nu_{52})(u_{25} + \beta_{25} - i\nu_{25})}{(u_{55} + \beta_{55} - \{g/\omega^2 d\}\beta_5 - i\nu_{55})}\right] \times \psi_2{}^{(1)} = -\psi_2{}^{(0)}(s)/L^2 \tag{53}$$

In solving these equations, Eq. (52) is to be solved first for $\psi_2{}^{(0)}$. With $\psi_2{}^{(0)}$ known, Eq. (53) can be solved for $\psi_2{}^{(1)}$. Next, with $\psi_2{}^{(0)}$ and $\psi_2{}^{(1)}$ known, Eq. (50) can be solved for $\psi_5{}^{(0)}$, and Eq. (51) can be solved for $\psi_5{}^{(1)}$.

In solving Eq. (52), let

$$(\pi/2)\frac{\rho d^2\omega^2}{T}\left[u_{22} + \beta_{22} - i\nu_{22} - \frac{2(u_{52} + \beta_{52} - i\nu_{52})(u_{25} + \beta_{25} - i\nu_{25})}{(u_{55} + \beta_{55} - \{g/\omega^2 d\}\beta_5 - i\nu_{55})}\right] = -\zeta_2{}^2 \tag{54}$$

and

$$-(\pi/2)\eta(s)\frac{\rho d^2\omega^2}{T} \times \left[c_2(s) - c_5(s)\frac{(u_{25} + \beta_{25} - i\nu)}{(u_{55} + \beta_{55} - \{g/\omega^2 d\}\beta_5 - i\nu_{55})}\right] = -f_2{}^{(0)}(s) \tag{55}$$

Hence,

$$d^2\psi_1{}^{(0)}/ds^2 - \zeta_2{}^2\psi_2{}^{(0)}(s) = f_2{}^{(0)}(s) \tag{56}$$

This is the inhomogeneous Helmholtz equation with the wavenumber, $i\zeta_2$, being a complex constant. At least one of the two solutions of the associated homogeneous equation grows exponentially in s. For this reason, a step-by-step numerical integration of the coupled equations for surge and roll cannot be used as a method of solution because roundoff errors will result in incorrect numerical divergence. Therefore, a numerical solution will be found by use of a Green's function satisfying

$$\partial^2 G_2/\partial s^2 - \zeta_2{}^2 G_2(s,s') = \delta(s - s') \tag{57}$$

where G_2 satisfies the same boundary conditions at the ends of the barrier as does $\psi_2{}^{(0)}$. The usual physical condition at an end of a barrier is that the barrier is connected to an anchor or a vessel by a long rope or cable. Under the assumption that the hydrodynamic force on the connection cable is small compared to the hydrodynamic force on the barrier, the boundary conditions at the ends of the barrier are

$$[d\psi_2{}^{(j)}/ds]_{s=0} = [d\psi_2{}^{(j)}/ds]_{s=L} = 0 \tag{58}$$

The Green's function satisfying Eqs. (57) and (58) with $\psi_2{}^{(0)}$ replaced by G is

$$G(s,s') = \frac{1}{2\zeta_2(1 - e^{2\zeta_2 L})} \times [e^{\zeta_2(s+s')} + e^{\zeta_2(2L-|s'-s|)} + e^{\zeta_2|s'-s|} + e^{\zeta_2(2L-s-s')}] \tag{59}$$

where ζ_2 is the square root of $\zeta_2{}^2$ that has a negative real part. The solution for $\psi_2{}^{(0)}$ is then given by

$$\psi_2{}^{(0)}(s) = \int_0^L f_2{}^{(0)}(s')G_2{}^{(0)}(s,s')ds' \tag{60}$$

Once $\psi_2{}^{(0)}$ is known, $\psi_2{}^{(1)}$ can be found from

$$\psi_2{}^{(1)}(s) = \int_0^L -\left(\frac{1}{L^2}\right)\psi_2{}^{(0)}(s')G_2(s,s')ds' \tag{61}$$

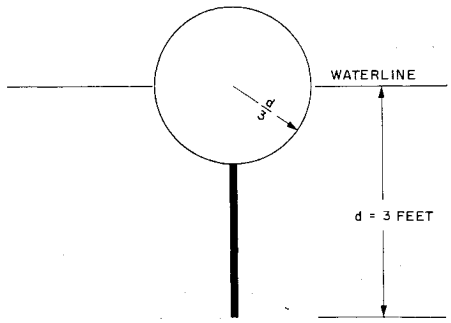

Fig. 3 Barrier cross section used for the sample calculations.

With $\psi_2^{(0)}$ and $\psi_2^{(1)}$ known, the solutions to Eqs. (50) and (51) are

$$\psi_5^{(0)}(s) = -\frac{[\eta c_{52}(s) - 2(u_{52} + \beta_{52} - i\nu_{52})\psi_2^{(0)}(s)]}{d[u_{55} + \beta_{55} - (g/\omega^2 d)\beta_5 - i\nu_{55}]} \quad (62)$$

and

$$\psi_5^{(1)}(s) = \frac{-2[u_{52} + \beta_{52} - i\nu_{52}]\psi_2^{(1)}(s)}{d[u_{55} + \beta_{55} - (g/\omega^2 d)B_5 - i\nu_{55}]} \quad (63)$$

For heave motions, the vertical forces are the wave force F_3^w, the "spring force" F_3^s, the motion force F_3^m, and the force due to tension in the barrier F_3^t where

$$f_3^t(s) = T(d^2\psi_3/ds^2) \quad (64)$$

Thus the equation for heave motion is

$$d^2\psi_3/ds^2 - \zeta_3^2\psi_3 = f_3(s) \quad (65)$$

where

$$\zeta_3^2 = -(\pi/2)(\rho d^2\omega^2/T)[u_{33} + \beta_{33} - (g/\omega^2 d)B_3 - i\nu_{33}] \quad (66)$$

and

$$f_3(s) = -(\pi/2)\eta(s)c_3(s)\rho d^2\omega^2/T \quad (67)$$

The solution to Eq. (65) is

$$\psi_3(s) = \int_0^L f_3(s')G_3(s,s')ds' \quad (68)$$

where $G_3(s,s')$ is given by Eq. (60) with G_2 replaced by G_3 and ζ_2 replaced by ζ_3.

Equations (60–63) and (68) are the approximate solutions for the barrier motions including two terms in the expansions for sway and roll motion in powers of ϵ. To obtain solutions in numerical form, values of the various parameters in the equations are required. Very little work has been completed in determining inertia, damping, and wave-force coefficients on barriers that are moving or are oblique to the wave direction. The Appendix gives some estimates of the coefficients for typical barriers in which the effects of the current on the coefficients are neglected.

4. Calculations

The motions of a barrier can be obtained by the straightforward numerical evaluation of Eqs. (60–63) and (68). In addition to the barrier motions, the difference between the wave elevation and the barrier heave, which is called the heave displacement difference, and the normal component of horizontal wave particle velocity relative to the swaying barrier, called the sway velocity difference, are of interest as they are related to the effectiveness of the barrier as a containment device. The complex amplitudes of these quantities can be obtained by subtraction of the appropriate complex amplitude of the barrier displacement or velocity from that of the wave. For structural purposes, the normal structural force as a result of tension in the barrier per unit length, F_2^t, is especially important because it can become quite large. Since the mass of most barriers is small compared to the added mass in sway, Eqs. (46) and (47) show that F_2^t is very nearly equal to the negative of the unsteady horizontal hydrodynamic force per unit length on the barrier.

Wave and motion force coefficients, spring constants, and barrier mass and inertia depend on the geometrical details of the barrier so that it is impossible to present any general quantitative results. However, a number of qualitative aspects of barrier forces and motions are common to a wide variety of barriers.

In order to demonstrate a few of these common aspects, calculations for a single barrier geometry are presented here. The barrier chosen has a length of 1000 ft and is comprised of a half-immersed cylinder with a one-foot radius above a flat plate having a height of two feet, thus giving a draft of three feet as shown in Fig. 3. The barrier is taken to be moored symmetrically with respect to the current direction so that Eqs. (9) and (10) hold. Wave propagation is chosen in the same direction as the current.

For the cross section chosen:

$$\beta_{11} = \tfrac{1}{9} \quad (69)$$

and

$$\beta_3 = 4/3\pi = 0.425 \quad (70)$$

Arbitrarily choosing the position of the center of mass to be at the middraft and the radius of gyration to be one foot gives

$$\beta_{55} = 0.0247 \quad (71)$$

$$\beta_{25} = 0.0 \quad (72)$$

and

$$\beta_5 = 0.233 \quad (73)$$

From the results of Robbins,[2]

$$C_d = 1.5 \quad (74)$$

Figure 4 shows the barrier configuration in a steady current [Eq. (7)] as well as the tension in the barrier [Eq. (12)] for various gap ratios for $\rho = 2$ slugs/ft^3 and $V = 3.16$ fps ($\sigma = 45$ slugs/sec^2).

Values of μ_{22}, ν_{22}, μ_{25}, ν_{25}, μ_{55}, ν_{55}, c_2, and c_5 are taken as those for a flat plate as given in the Appendix. μ_{33} and ν_{33} for a floating circular half cylinder are given by Porter.[7] c_3 is then determined by applying the Haskind[8] relations to Porter's results. Table 1 lists these coefficients.

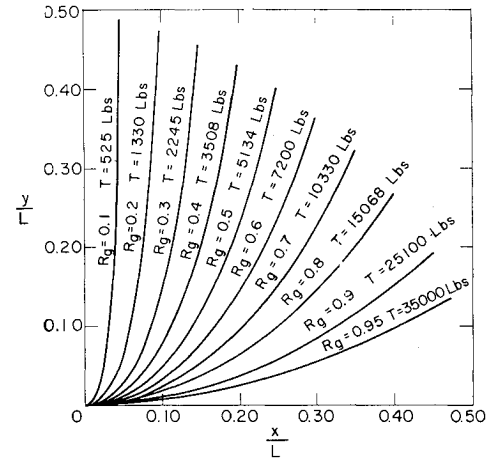

Fig. 4 An example of steady barrier configurations for various gap ratios for the case of $\tau = 45$ slugs/sec^2. Note the large tensions associated with large values of the gap ratio.

Table 1 Coefficients for barrier used in calculations

kd	μ_{22}	ν_{22}	μ_{55}	ν_{55}	μ_{25}	ν_{25}	μ_{33}	ν_{33}	ω	C_2	$arg(C_2)$	C_5	$arg(C_5)$	C_3	$arg(C_3)$
0.05	1.050	0.005	0.071	0.0003	0.083	0.001	0.327	0.260	0.734	1.04	1.560	0.16	1.560	8.14	0.01
0.1	1.104	0.020	0.074	0.0006	0.091	0.003	0.274	0.241	1.030	1.08	1.555	0.16	1.555	3.94	0.03
0.2	1.233	0.085	0.079	0.0013	0.110	0.009	0.194	0.212	1.470	1.16	1.505	0.20	1.505	1.84	0.07
0.3	1.369	0.214	0.081	0.0037	0.129	0.018	0.137	0.193	1.796	1.23	1.416	0.23	1.416	1.17	0.11
0.4	1.471	0.420	0.082	0.0086	0.140	0.033	0.090	0.175	2.071	1.31	1.286	0.26	1.286	0.836	0.14
0.5	1.475	0.710	0.082	0.016	0.139	0.060	0.110	0.161	2.319	1.35	1.116	0.28	1.116	0.640	0.18
0.6	1.336	1.007	0.080	0.024	0.135	0.118	0.103	0.149	2.540	1.33	0.923	0.29	0.923	0.515	0.22
0.7	1.108	1.190	0.078	0.029	0.118	0.142	0.097	0.138	2.746	1.24	0.732	0.27	0.732	0.424	0.26
0.8	0.806	1.249	0.075	0.036	0.084	0.146	0.092	0.130	2.933	1.12	0.565	0.27	0.565	0.361	0.29
1.0	0.401	1.121	0.070	0.039	0.039	0.143	0.083	0.115	3.277	0.85	0.327	0.22	0.327	0.271	0.37
1.5	0.106	0.600	0.057	0.035	−0.010	0.108	0.071	0.090	4.020	0.44	0.090	0.14	0.090	0.249	0.56
2.0	0.084	0.451	0.049	0.031	−0.023	0.081	0.066	0.070	4.638	0.27	0.028	0.10	0.028	0.145	0.74
3.0	0.128	0.244	0.040	0.027	−0.033	0.05	0.067	0.045	5.675	0.13	0.003	0.06	0.003	0.085	1.12
4.0	0.176	0.120	0.036	0.026	−0.034	0.039	0.071	0.028	6.545	0.08	0.001	0.05	0.001	0.051	1.49
5.0	0.214	0.099	0.029	0.019	−0.035	0.027	0.122	0.017	7.323	0.05	0.000	0.03	0.000	0.033	1.89

Determination of the coefficients in the manner described above neglects the roll moment on the cylinder due to the waves. Garrison[9] has calculated wave moments on a plate lying on the surface. For the barrier considered here, the wave moment on a surface plate as wide as the cylinder diameter, is small compared to the wave moment on the vertical part of the barrier. Hydrodynamic interactions between the effects of the vertical part of the barrier and the buoyant part have not been accounted for. However, the coefficients obtained above should be representative of those for a barrier cross section very similar to that shown in Fig. 4.

Figure 5 shows the complex amplitude of the roll and sway motions along the barrier as well as the sway velocity difference and the mechanical force $f_2{}^t$ for $kd = 0.4$ and $R_g = 0.6$. The similarity in the shape of the curves for the roll amplitude and for the sway velocity difference should be noted. Analysis of Eq. (62) and the coefficients in this equation indicates that this similarity should occur for small values of kd. This indicates the importance of cross-coupling between sway and roll in determining the roll motion. As indicated in the figure, $\psi_2{}^{(1)}$ and $\psi_5{}^{(1)}$ are negligibly small in this example.

Figure 6 shows the complex amplitudes of the heave motion ψ_3 and the heave displacement difference. An important error occurs here due to the fact that the immersed shape of the buoyant cylinder changes when the displacement difference is not equal to zero. In fact, if the displacement difference were as shown in the figure, the cylinder would be totally submerged over part of each wave cycle and be totally above the surface over a different part of each wave cycle over most of the barrier in moderate seas. This submergence or rising above the surface does not occur over all parts of the barrier simultaneously, but travels in waves along the barrier. Because of the error introduced here by the assumption of small waves and motions, heave results can only be interpreted qualitatively when the heave displacement difference is not small.

Figure 7 shows the maximum complex amplitudes of roll angle, the sway velocity difference, the heave displacement difference and the horizontal mechanical force f^t for $R_g = 0.6$ as functions of kd. Of special importance is the fact that f^t, which is very nearly equal to the complex amplitude of the unsteady hydrodynamic force per unit length on the barrier (see Sec. 3), can be an order of magnitude larger than the steady current force on the barrier under conditions in which barriers are normally used.

Figure 8 shows maximum values of the roll angle, the heave displacement difference, the sway velocity difference and $f_2{}^t$ as functions of the gap ratio for $R_g = 0.4$. The results of this figure indicate that if $kd = 0.4$ for the dominant waves, R_g should be set between 0.4 and 0.45 for optimum operation of the barrier.

5. Discussion

The numerical calculations of Sec. 4 indicate a number of generalities about floating barriers. If a barrier is to operate as an effective containment device, it is desirable that it follow the horizontal motion of the fluid particles normal to itself to

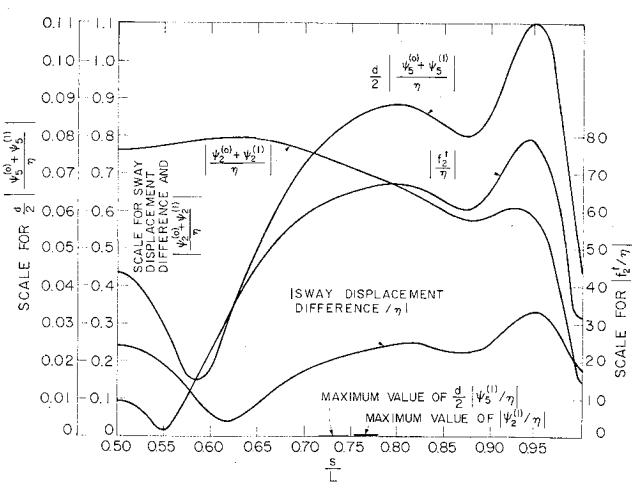

Fig. 5 Roll and sway motion, sway velocity difference, mechanical force magnitudes on the barrier used for sample calculations; $kd = 0.4$, $R_g = 0.6$, $\alpha = \pi/2$ (waves propagating in the same direction as the current).

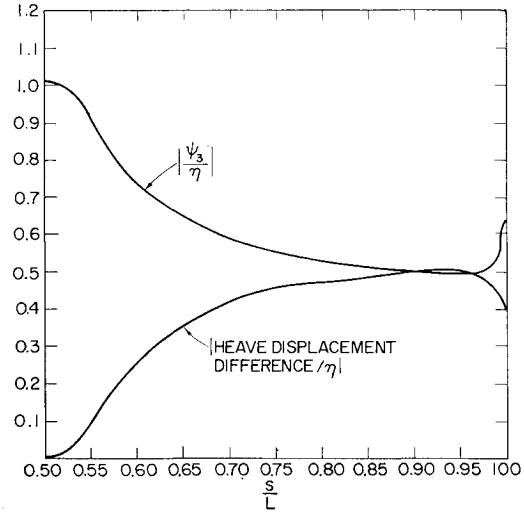

Fig. 6 Heave motion and heave displacement difference magnitudes on the barrier used in the sample calculations; $kd = 0.4$, $R_g = 0.6$, $\alpha = -\pi/2$.

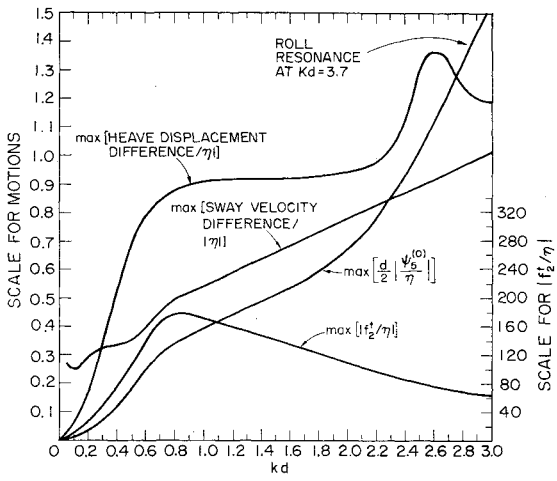

Fig. 7 Maximum values of the magnitudes of heave displacement difference, sway displacement difference and horizontal mechanical force on the barrier as functions of kd for $R_g = 0.6$. This figure was made by determining the values of the various quantities along the barrier at numerous values of kd. Then the maximum values of each quantity were plotted. Because of the wave-like character of the quantities, the maxima occur at different positions on the barrier for different values of kd. Any maximum occurring nearer the end of the barrier than $L/20$ was disregarded.

avoid high relative fluid velocities that could sweep the material being contained over or under the barrier. Figure 5 indicates other reasons for attempting to achieve good sway response. Roll motions tend to follow the relative sway velocity and since containment failure can be caused by large rolling, it is desirable to minimize the roll. High relative sway velocities also lead to high horizontal unsteady hydrodynamic forces on the barrier. Figures 5 and 7 indicate that these forces can be much larger than the steady current forces in usual currents. An assumption for this work is that the

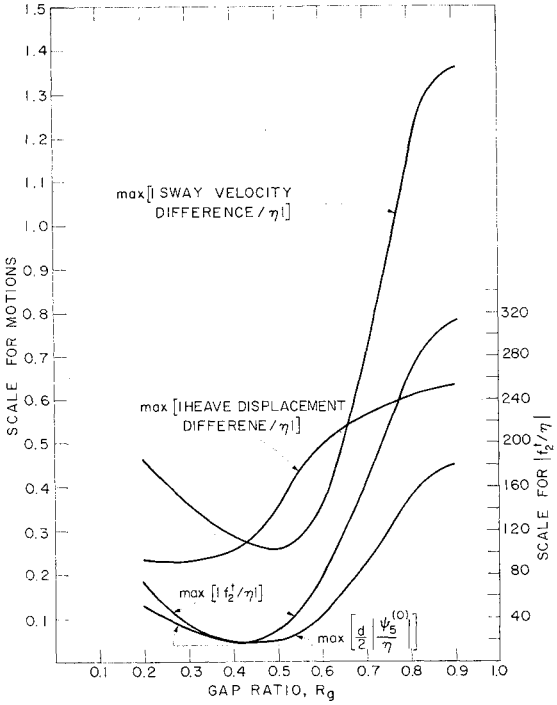

Fig. 8 Maximum values of the magnitudes of roll angles, heave displacement difference, sway velocity difference and horizontal mechanical force on the barrier as functions of R_g for $kd = 0.4$. This figure was made in the same manner as Fig. 7, but with kd held fixed and R_g being varied.

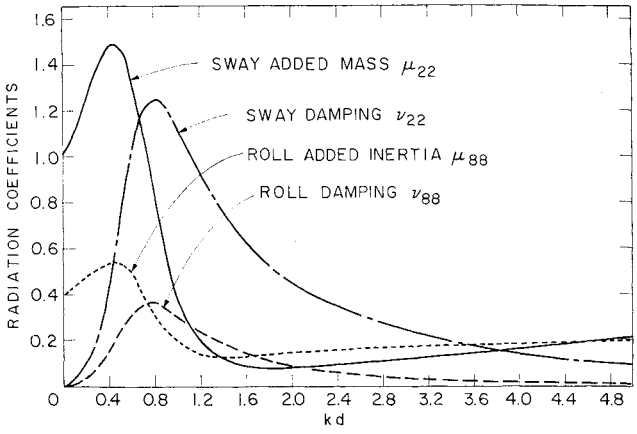

Fig. 9 Motion coefficients of a flat plate for sway and roll about the waterline as given by Kotik.[11]

barrier tension is constant. If in fact the tension increases when the barrier is extended longitudinally, the sway response will be degraded. In the case of long crested seas of large wavelength, a single wave affects almost the entire barrier at any given time. In this case, barrier compliance can be provided in its end attachments. However, in short crested confused seas, the compliance must be distributed throughout the barrier which, from the standpoint of design, is much more difficult to achieve. Since perfect sway response is impossible to achieve and the forces caused by relative unsteady sway velocity are so large, barriers must be much stronger than the forces caused by a steady current indicate if they are to survive in the presence of waves.

Effective containment with a practical barrier is dependent on the barrier following the vertical surface elevation in the waves, i.e., the heave displacement difference must be small. Otherwise, the barrier must have a large vertical plate above the waterline as well as being extraordinarily deep. The increased depth would raise the tension, which in turn impedes sway response. The heave response, considered as a function of kd, is resonant with a maximum at that value of kd where the real part of f_3^m is exactly opposite to f_3^s. The frequency associated with this value of kd will be called the natural frequency. In the absence of damping effects, free oscillations in heave would not occur exactly at the natural frequency here because of the effect of the barrier tension force f_3^t. However, this restoring force is significantly less than the spring force f_3^s for most practical barrier configurations so that free oscillations in heave in the absence of damping would occur at a frequency nearly equal to the natural frequency. As with any resonant system, accurate following of the surface elevation can only occur when the significant wave frequencies are much less than the natural frequency of the barrier in heave. This yields the design condition that the natural frequency of the barrier in heave should be as high as possible. This implies that the spring constant B_3 should be large and the barrier mass B_{33} and the added mass in heave μ_{33} should be small. Altering a barrier configuration so as to increase B_3 causes rather large increases in μ_{33}. Therefore, it is necessary to make the barrier as light as possible and then find a configuration for the buoyant part that maximizes the natural frequency in heave.

The roll response is also resonant, and in the case considered here where there is no roll restoring force due to barrier tension, the roll response is exactly that of a second-order system. As was the case with heave, effective containment requires that the natural frequency in roll be much larger than the significant wave frequencies.

The problem of determining barrier motions in the presence of waves and currents is almost identical to the problem of determining the motions of a long towed cable in waves.

The only significant difference is that the cable problem has the added difficulty of a variation in tension along the cable. Attempts at solution of the cable motion problem by direct numerical integration frequently fail because of a divergent characteristic solution to the equation of motion. The basis for this divergent solution is shown here in Sec. 3 for the case of constant tension. The method of solution used here avoids the difficulties of numerical divergence and could be used in the cable problem. However, the Green's Function for the cable problem is not only more complicated than that of the barrier problem [Eq. (59)], but it cannot be specified a priori because it depends on the distribution of tension in the cable. A simplified method of solution to the cable problem in some cases could be obtained by exploiting the fact that cables are often used to tow a body that has a large drag. For these cases, the tension is a slowly varying function of distance along the cable. Also, the steady-state curvature of the cable is small so that the unsteady curvature of the cable is accurately approximated by

$$\text{curvature} = d^2\zeta/ds^2 \tag{75}$$

where ζ is the complex amplitude of the cable displacement. Let the tension be given by

$$T = T^{(0)} + \epsilon T^{(1)}(s) \tag{76}$$

and assume that ζ can be expanded as

$$\zeta = \zeta^{(0)} + \epsilon\zeta^{(1)} + \epsilon^2\zeta^{(2)} \ldots \tag{77}$$

The complex amplitude of the normal force due to tension is then

$$f^m(s) = T^{(0)}\zeta^{(0)}(s) + \epsilon[T^{(1)}(s)\zeta^{(0)}(s) + T^{(0)}\zeta^{(1)}(s)] + \epsilon^2[T^{(1)}(s)\zeta^{(1)}(s) + T^{(0)}\zeta^{(2)}(s)] + \ldots \tag{78}$$

Solution of the equation of motion in each power of ϵ can be carried out by the use of the Green's function given by Eq. (59). In fact, the solution for $\xi^{(0)}$ is exactly the same as the solution for $\psi_2^{(0)}$, given in this paper by Eq. (60). The $\xi^{(n)}$'s can be sequentially determined by Eq. (60) with $G_2^{(0)}$ appropriately altered.

Appendix: Wave and Motion Force Coefficients for a Barrier in Waves and Currents

The approximate theory developed in Sec. 3 requires specification of the inertia, damping, and wave-force coefficients for a long, straight section of barrier at an arbitrary angle to the waves in the presence of a current. Essentially, no work on the problem of determining these coefficients has been completed at this time. In most cases, data only exists in the absence of a steady current with wave-force coefficients available for a section of barrier with its centerplane normal to the wave direction. The neglect of the effect of the current results in neglecting the effect of the current on the wave encounter frequency. This effect is truly negligible in most barrier calculations because the phase velocity of the waves of interest is an order of magnitude larger than the current velocities usually encountered. An effect causing more concern is that of flow separation near the lowest extremity of the barrier, since most barrier configurations have a sharp lower edge. It has been shown by Keulegan and Carpenter[6] that the effects of flow separation on forces are strongest when fluid particles travel distances that are large compared to cross-sectional body dimensions between times at which the flow direction reverses. In the absence of a current, the flow direction reverses twice during each wave period. However, in many cases the current velocity is of the same order of magnitude as the fluid particle velocity due to the wave, so that horizontal velocity reversals may not occur. This effect appears to be the largest possible source of error in neglecting the effect of the current on the force coefficients.

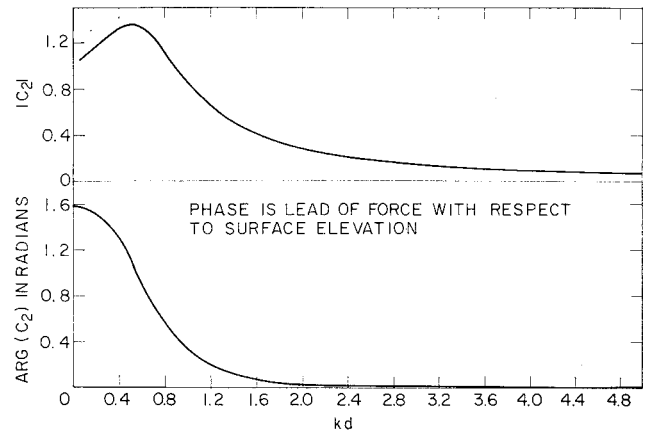

Fig. 10 Wave sway force coefficient on a flat plate, c_2.

Most barriers are comprised of a thin, vertical member which serves as most of the barrier, with flotation attached near the upper portion of the barrier and ballast near the lower portion. For structures of such a cross section, the sway and roll force coefficients can be approximated by those for a flat plate of the same draft. Ursell[10] has analyzed the fluid motion generated by a surface-piercing, two-dimensional plate rolling about an arbitrary horizontal axis. Kotik[11] has used the results of this analysis to determine the damping coefficients $\nu_{22}(kd)$ and $\nu_{88}(kd)$. He also determined the inertia coefficients $\mu_{22}(kd)$ and $\mu_{88}(kd)$ by application of the Kramers-Kronig relations to the damping coefficient functions. The subscript 8 refers to roll about the waterline. For an explanation of the Kramers-Kronig relations, see Ogilvie.[12] These coefficients are shown in Fig. 9.

Formulae for the above coefficients, as well as for μ_{28}, μ_{82}, ν_{28}, and ν_{82}, were determined by Haskind[13] through a method of analysis quite different than that used by Ursell.[10] Evaluations of Haskind's formulae have not yielded satisfactory results, and his work is currently under study.

The wave-force coefficients $c_2(kd)$ and $c_8(kd)$ can be determined in terms of $\nu_{22}(kd)$ and $\nu_{88}(kd)$ by means of the Haskind relations and knowledge of the far-field wave phase resulting from appropriate motions of the plate (see, e.g., Newman[8]).

If the rest position of the centerplane of the plate is at $x = 0$, and the plate performs a motion in its jth degree of freedom having the time dependence $e^{i\omega t}$, the surface elevation as $x \to -\infty$ will be of the form

$$\lim_{x\to-\infty} N_j(x,t) = \eta_j e^{i(\omega t + \kappa x)} \tag{A1}$$

Since deep water waves are being considered,

$$\omega^2 = kg \tag{A2}$$

The far-field wave phase $\delta_j(kd)$ is defined as

$$\delta_j(kd) = Arg\eta_j \tag{A3}$$

The Haskind relations[8] yield

$$c_j{}^n = (1/kd)(2\nu_{jj}/\pi)^{1/2}e^{i(\pi/2+\delta_j)}, j = 2,3 \tag{A4}$$

$$c_j{}^n = (1/kd)(4\nu_{88}/\pi)^{1/2}e^{i(\pi/2+\delta_j)}, j = 5,8 \tag{A5}$$

where $c_j{}^n$ is the coefficient for normal incidence of the wave. Values of δ_2 and δ_8 are given by Kotik.[11] c_2 and c_8, as determined from Eqs. (A4) and (A5) are shown in Figs. 10 and 11.

The force coefficients about the middraft are obtained as follows. For an incident wave of half amplitude η, the surge force is

$$F_2{}^w = (\pi/2)\rho d^2\omega^2\eta c_2{}^n e^{i\omega t} \tag{A6}$$

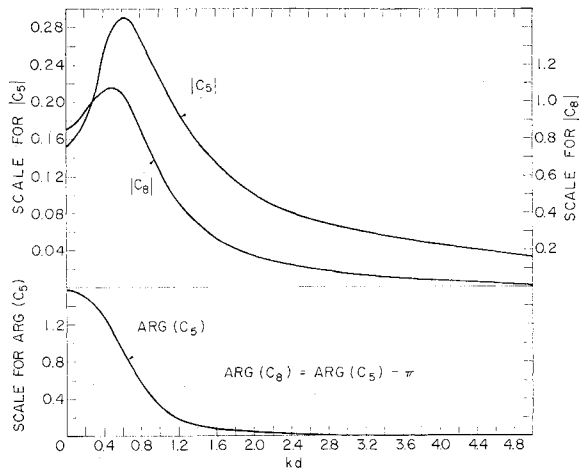

Fig. 11 Wave roll moment coefficients on a flat plate c_5 and c_8.

and the roll moment about the waterline is

$$F_8^w = (\pi/4)\rho d^3\omega^2\eta c_8^n e^{i\omega t} \quad \text{(A7)}$$

c_2 and c_8 are known (Figs. 10 and 11). The roll moment about the middraft is

$$F_5^w = (\pi/4)\rho d^3\omega^2\eta(c_2^n + c_8^n)e^{i\omega t} \quad \text{(A8)}$$

Thus, from Eqs. (14) and (A7),

$$c_5^n(kd) = c_2^n(kd) + c_8^n(kd) \quad \text{(A9)}$$

$c_5^n(kd)$ is shown in Fig. 11.

$\nu_{55}(kd)$ has been obtained from c_5^n by the Haskind relation, Eq. (A5), and is shown in Fig. 12.

In order to determine μ_{55}, the Kramers-Kronig relations[12] will be used in the following form:

$$\mu_{55}(kd) - \mu_{55}(\infty) = (1/\pi)\int_0^\infty \frac{\nu_{55}(q)}{q - kd}\,dq \quad \text{(A10)}$$

Since $\nu_{55}(kd)$ is known from Eq. (A5), $\mu_{55}(kd)$ can be determined from Eq. (A8) if $\mu_{55}(\infty)$ is known. For a plate rolling about its middraft with angle $\Psi_5 = \psi_5 e^{i\omega t}$, the high frequency limit for the velocity potential on the plate can be shown to be

$$\lim_{\omega\to\infty}\phi_5(z) = -(i/\pi)\omega\psi_5 z\{(\pi/2)(d^2 - z^2)^{1/2} + d\log[d + (d^2 - z^2)^{1/2}]/[-z]\}e^{i\omega t},\ -d/2 < y < 0 \quad \text{(A11)}$$

The pressure on the plate is given by

$$P_5(y,t) = -\rho(\partial\phi_5/\partial t) \quad \text{(A12)}$$

$\lim_{\omega\to\infty}\mu_{55}$ is given by

$$\lim_{\omega\to\infty}\mu_{55} = -4/\pi d^4\omega^2\theta_o\int_{-d}^0 (z + d/2)|P_5(z,t)|dz \quad \text{(A13)}$$

Carrying out the indicated integration gives

$$\mu_{55}(\infty) = \tfrac{1}{4} - 2/\pi^2 = 0.04736 \quad \text{(A14)}$$

Using this result, $\mu_{55}(kd)$ was found from Eq. (A10) by means of a digital computer program and is shown in Fig. 12.

Now the cross-coupling coefficients μ_{25}, ν_{25}, μ_{52}, and ν_{52} can be determined. This is done by means of a consideration of a rolling motion of the plate about the mean waterline as shown in Fig. 13. The motion is

$$\Psi_8 = \psi_8 e^{i\omega t} \quad \text{(A15)}$$

This results in a roll moment about the waterline of

$$f_8^n = -(\pi/4)\rho d^4\omega^2\psi_8(\mu_{88} - i\nu_{88}) \quad \text{(A16)}$$

The motion given by Eq. (A15) can be constructed from roll about the middraft plus sway (Fig. 13). The roll about the middraft is

$$\psi_5 = \psi_8 \quad \text{(A17)}$$

and the sway is

$$\psi_2 = -d/2\psi_8 \quad \text{(A18)}$$

The sum of these two motions results in a sway force of

$$f_2^m = -(\pi/4)\rho d^3\omega^2\psi_8(\mu_{22} - i\nu_{22}) + (\pi/2)\rho d^3\omega^2\psi_8(\mu_{25} - i\nu_{25}) \quad \text{(A19)}$$

and a moment about the middraft of

$$f_5 = -(\pi/4)\rho d^4\omega^2\psi_8(\mu_{52} - i\nu_{52}) + (\pi/4)\rho d^4\omega^2\psi_8(\mu_{55} - i\nu_{55}) \quad \text{(A20)}$$

This force and moment can be resolved about the waterline, giving

$$f_8^m = f_5^m - (d/2)f_2^m = (\pi/4)\rho d^4\omega^2\psi_8[(\mu_{22} - i\nu_{22})/2 + (\mu_{55} - i\nu_{55}) - (\mu_{25} - i\nu_{25}) - (\mu_{52} - i\nu_{52})] \quad \text{(A21)}$$

It has been shown by Haskind[13] and Newman and Timann[14] that

$$\mu_{52} = \mu_{25} \quad \text{(A22)}$$

and

$$\nu_{52} = \nu_{25} \quad \text{(A23)}$$

Therefore,

$$f_8^m = (\pi/4)\rho d^4\omega^2\psi_8[(\mu_{22} - i\nu_{22})/2 + (\mu_{55} - i\nu_{55}) - 2(\mu_{25} - i\nu_{25})] \quad \text{(A24)}$$

Comparison of Eq. (A21) with Eq. (A24) yields

$$\mu_{25}(kd) = (\tfrac{1}{2})[\mu_{22}(kd)/2 + \mu_{55}(kd) - \mu_{88}(kd)] \quad \text{(A25)}$$

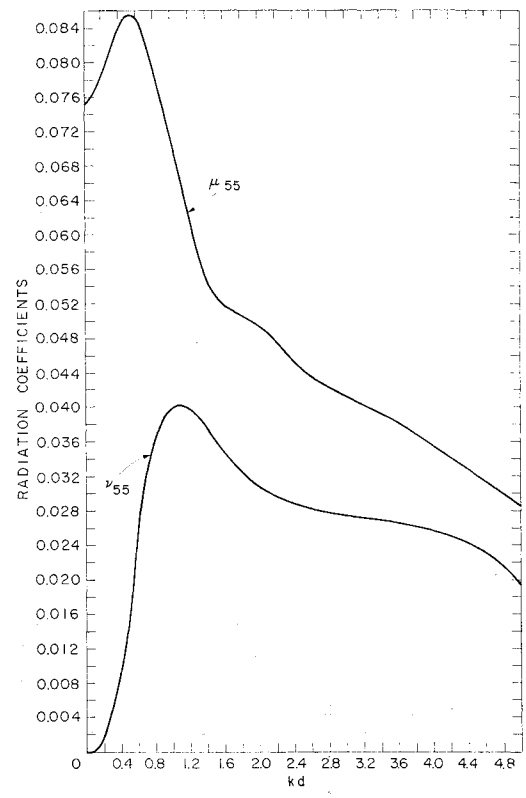

Fig. 12 Motion coefficients for a flat plate rolling about its middraft.

and

$$\nu_{25}(kd) = (\tfrac{1}{2})[\nu_{22}(kd)/2 + \nu_{55}(kd) - \nu_{88}(kd)] \quad \text{(A26)}$$

$\mu_{25}(kd)$ and $\nu_{25}(kd)$ are shown in Fig. 14.

Figures 10 and 11 give the wave-force coefficients for sway and roll for waves having normal incidence. Because of a lack of knowledge of these coefficients for oblique incidence, an approximation based on the coefficients at normal incidence is used. The approximation recommended is

$$c_j = c_j^n \sin(\theta_o - \alpha), \quad j = 2,3,8 \quad \text{(A27)}$$

where α is the angle between the direction of wave propagation and the x axis. There are a number of reasons for this choice of an approximation. To the extent that fluid forces depend only on local wave particle velocities normal to the barrier, the approximation is exact. Also, the approximation is correct for the angle between the propagation vector and the normal to the barrier being any integer multiple of $\pi/2$ rads.

Values for the heave-force coefficients μ_{33}, ν_{33}, and c_3 depend on the geometrical details of the barrier and must be determined for each particular case. μ_{33} and ν_{33} for a number of two-dimensional cylindrical forms are given by Porter.[7] He also gives $\delta_3(ka)$ for a circular cylinder as does Ursell,[15] so that c_3^n can be determined from the Haskind relation [Eq. (A4)].

The vertical wave force on a flat plate lying on the surface (finite dock) in oblique waves has been determined theoretically by Garrison.[9] He found that the heave force was essentially independent of wave incidence angles for departures from normal incidence less than 75° and values of k times the plate width less than 0.4. For the barrier used in the examples of Sec. 4, the width of the waterline was one-third of the depth. If the independence of surge force on incidence angle found for the plate lying on the surface applies to buoyant bodies of the same waterplane width, wave heave forces on the barrier in the examples would be independent of angle for kd less than 1.2. This includes all waves of interest. Garrison's results are quite reasonable since most of the heave force on a body in long waves is a result of simple buoyancy when the water level changes in a wave. For these reasons the recommended approximation for c_3 is

$$c_3 = c_3^n \quad \text{(A28)}$$

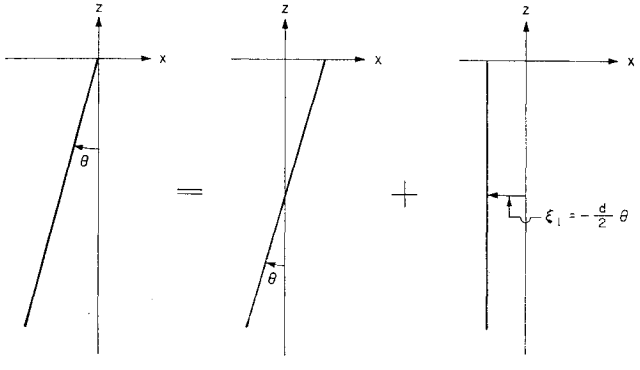

Fig. 13 Motion of a plate used for a determination of the cross-coupling coefficients between sway and roll. The roll motion about the waterline shown in the left diagram can be represented as the sum of the roll motion about the middraft shown in the center diagram and the sway shown in the right diagram. The waterline is at $Z = 0$ and the plate has draft d.

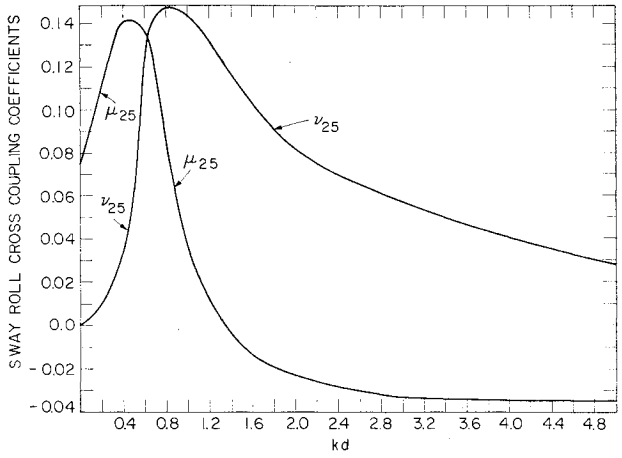

Fig. 14 Hydrodynamic cross-coupling coefficients between sway and roll.

References

[1] Hoult, D. P., "Conference of Oil Spills by Physical and Air Barriers," Annual Meeting of the American Institute of Chemical Engineers, Puerto Rico, 1970.

[2] Robbins, R., "The Oil Boom in a Current," M.S. thesis, 1970, Dept. of Electrical Engineering, M.I.T., Cambridge, Mass.

[3] Eames, M. C., "Steady State Theory of Towing Cables," *Quarterly Transactions of the Royal Institution of Naval Architects*, Vol. 110, No. 2, 1968, pp. 185–206.

[4] Springston, G. B., "Generalized Hydrodynamic Loading Functions for Bare and Faired Cables in Two-Dimensional Steady-State Cable Configurations," Rept. 2424, 1967, Naval Ship Research and Development Center, Hydrodynamics Lab., Washington, D. C.

[5] Drake, S. H., "Dynamics of an Oil Containment Boom in a Wave Field," M.S. thesis, June 1970, Dept. of Mechanical Engineering, M.I.T., Cambridge, Mass.

[6] Keulegan, G. H. and Carpenter, L. H., "Forces on Cylinders and Plates in an Oscillating Fluid," Research Paper 2857, *Journal of Research of the National Bureau of Standards*, Vol. 60, No. 5, 1958, pp. 423–440.

[7] Porter, W. R., "Pressure Distributions, Added-Mass, and Damping Coefficients for Cylinders Oscillating in a Free Surface," Series 82, Issue 16, 1960, Institute of Engineering Research, Univ. of California, Berkeley, Calif.

[8] Newman, J. N., "The Exciting Forces on Fixed Bodies in Waves," *Journal of Ship Research*, Vol. 6, No. 3, 1962, pp. 10–17.

[9] Garrison, C. J., "On the Interaction of an Infinite Shallow Draft Cylinder Oscillating at the Free Surface with a Trail of Oblique Waves," *Journal of Fluid Mechanics*, Vol. 39, Pt. 2, 1969, pp. 227–255.

[10] Ursell, F., "On the Waves Due to the Rolling of a Ship," *Quarterly Journal of Mechanics and Applied Mathematics*, Vol. 1, 1948, pp. 246–252.

[11] Kotik, J., "Damping and Inertia Coefficients for a Rolling or Swaying Vertical Strip," *Journal of Ship Research*, Vol. 7, No. 2, Oct. 1963, pp. 19–23.

[12] Ogilvie, T. F., "Recent Progress Toward the Understanding and Prediction of Ship Motions," *Fifth Symposium on Naval Hydrodynamics*, Vol. ACR-112, 1964, Office of Naval Research, Dept. of the Navy, Washington, D. C.

[13] Haskind, M. D., "The Radiation and Diffraction of Surface Waves from a Vertically Floating Plate," *Prikladnaia Matematiki i Mekhanika*, Vol. 23, No. 3, 1959, pp. 546–556.

[14] Timman, R. and Newman, J. N., "The Coupled Damping Coefficients of a Symmetric Ship," *Journal of Ship Research*, Vol. 5, No. 4, 1962, pp. 1–7.

[15] Ursell, F., "On the Heaving Motion of a Circular Cylinder on the Surface of a Fluid," *Quarterly Journal of Applied Mathematics*, Vol. 2, Pt. 2, 1949, pp. 218–231.